04

Particles combustion of interaction of a microwave pulse of a gyrotron with a mixture of metal/dielectric powders

© Z.A. Zakletskii, N.G. Gusein-zade, D.V. Malakhov, L.V. Badyanova, E.V. Voronova, V.D. Stepakhin

Prokhorov Institute of General Physics, Russian Academy of Sciences,
119991 Moscow, Russia
e-mail: fiveziggen@gmail.com

Received May 16, 2023
Revised July 17, 2023
Accepted July 20, 2023

As a result of interaction under normal conditions in an air atmosphere of a microwave pulse of a gyrotron with a mixture of Al/Al_2O_3 powders, ceramic particles of morphology microprocesses are synthesized. A variant of a multi-stage process for the development of physical and chemical processes in a reactor, taking into account ignition. After the end of the microwave pulse, a cloud is observed consisting of hot aluminum oxide particles and burning aluminum particles. A certain influence of the combustion process of aluminum particles on the products of plasma-chemical synthesis. The paper also determines the average velocity of particles from the powder mixture, the burning time of aluminum particles, the surface temperature of the particles of the powder mixture, and the temperature of the gaseous medium in the upper part of the plasma-chemical reactor.

Keywords: Plasma, combustion particles and flame, microwave, materials.

DOI: 10.61011/TP.2023.09.57357.127-23

Introduction

Physicochemical processes occurring during heterogeneous combustion of micro- and nanoparticles make it possible to synthesize materials with new mechanical, thermodynamic, catalytic, and electromagnetic properties [1]. Of particular interest are the combustion reactions of metals in various oxidizing media with the formation of oxides, spinels, and nitrided particles [2].

The method of flame-spray pyrolysis (flame-spray pyrolysis, FSP) in a gaseous [3–4] environment, in which particulate aerosol is atomized through a burner flame or plasma torch, is widely used. In such studies, plasma with high gas temperature up to 10^4 K is generated by a high-frequency field or electric arc in the gas flow. During the time of particle interaction with the plasma plume — a few ms — the particle has time to undergo phase and morphological changes.

The main mechanism of particle formation and modification in FSP is the process of evaporation of a small-scale fraction of metallic particles and condensation of its vapors on larger oxide or metallic particles [5]. When oxidizing medium (oxygen, air) is used as a plasma-forming gas, processes of ignition of metal particles occur after passing the high-temperature area of the plume. As a result, instead of evaporation, the particle surface begins to oxidize with additional energy release, which can significantly affect the thermo-physical parameters of particle fusion. Therefore, it is necessary to accurately determine the characteristic ignition times of the particles and plasma treatment in experiments conducted in an oxidizing medium.

Our previous works [6–8] were devoted to high-temperature synthesis of substances in the interaction of metal-dielectric powders with pulsed gyrotron radiation. The synthesis conditions were similar to FSP, we observed a layer dense enough for a low-temperature plasma (electron density $n_e > 10^{14}\,\mathrm{cm}^{-3}$) with a gas temperature of more than 3000 K, with which flying powder particles interacted for more than 1 ms. Most of our experiments with an open upper boundary were performed in a nitrogen atmosphere at reduced pressure, or in an air atmosphere.

When synthesized by the method presented in this work, complex metal-dielectric particles are formed, which are widely used in the chemical industry when used as catalysts in various reactions involving liquid organic hydrogen carriers. However, when particles are synthesized in an oxidizing medium, combustion products of the initial metal particles may be observed in the reaction products, which will reduce the amount of synthesized material, thereby affecting the activity of the particle-catalysts in chemical reactions.

In the present work, we decided to investigate the ignition and combustion of aluminum metal particles, to obtain gas temperature values in the upper area of the reactor where the influence of the plasma discharge is minimal, and to perform optical measurements inside the plasma-chemical reactor in order to obtain additional information on the stages of plasma-chemical synthesis and on the influence of the combustion process on the synthesis products.

1. Materials and technique of experiment

The presence of both metal and dielectric is necessary for the development of discharge in our experiments. Mixture Al/Al_2O_3 was chosen based on the known extensive research on the ignition and combustion of aluminum particles [9]. The high-temperature phase α-Al_2O_3, was chosen as the oxide to avoid additional chemical transformations.

In experiments, a mixture of powders of metallic aluminium at a concentration of 20% of the total mass of 1.54 g and α-phase aluminium oxide powder was used. The powders consisted of micron-sized aluminum particles (GOST PA-4, linear particle size from 1 to 100 μm, purity 99.5%), and aluminum oxide (nominal particle diameter up to 50 μm, purity 99.8%). The shape and size of the particles were further investigated using a scanning election microscope (EVO 10 from GmbH Zeiss Microscopy (Jena, Germany)) (Fig. 1). Most aluminium particles are irregularly shaped, whereas aluminium oxide has a spherical shape with sharp protrusions of submicron size.

The experimental setup (Fig. 2) consists of a powerful pulsed gyrotron, a plasma chemical reactor where particle synthesis takes place, microwave diagnostics and optical diagnostics consisting of a set of spectrometers, a photodetector and fast cameras.

1.1. Gyrotron

The plasma chemical reactor uses pulsed microwave radiation from a gyrotron to initiate the synthesis of new particles. Gyrotron (manufacturer GICOM, Nizhny Novgorod, Russia) generates microwave radiation at a given frequency of 75.0 GHz with a power up to 600 kW, the duration of one microwave pulse can be set from 1 to 20 ms. The beam intensity distribution at the output window of the gyrotron is approximated by a Gaussian. After the output window of the gyrotron, the microwave radiation enters the tap, where a small part of the microwave power of the beam is reflected to the diagnostic detector ($mw\ in$, Fig. 2). The tap is a quartz cube with a mica quarter-wave plate placed in the center at an 45° angle. After passing the tap, the beam hits the mirror and is focused onto the bottom window of the reactor. The diameter of the Gaussian beam arriving at the bottom quartz plate of the reactor is 5 cm. After the reactor, the microwave radiation enters a section with ceramic absorbers, in the center of which is located a microwave detector of the elapsed radiation ($mw\ tsm$, Fig. 2). In the case of discharge initiation, part of the microwave energy of the beam will be reflected towards the beam into the tap, from where it will fall on the microwave detector of reflected radiation ($mw\ ref$, Fig. 2).

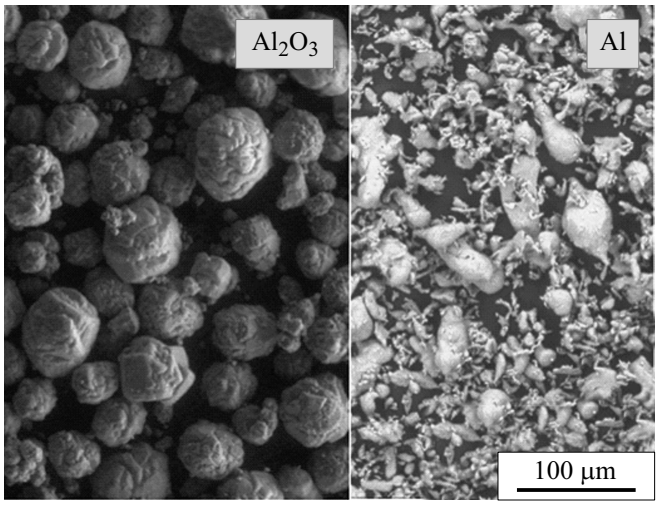

Figure 1. SEM images of initial aluminum and aluminum oxide particles in α-phase

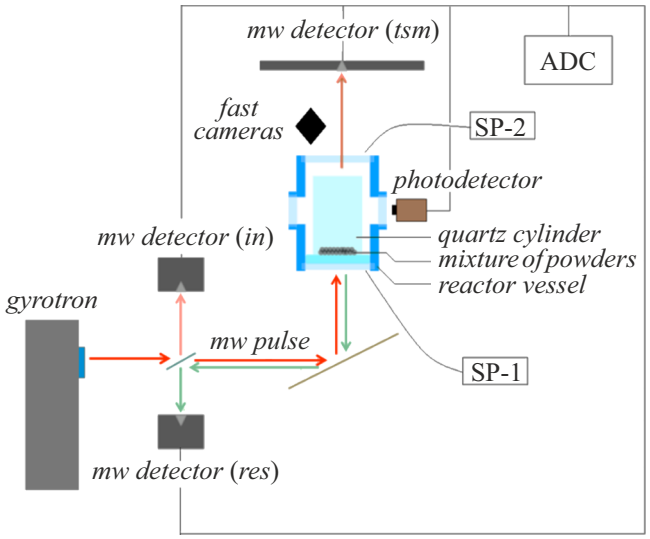

Figure 2. Experimental setup for plasma chemical synthesis of substances by interaction of microwave gyrotron pulse with a mixture of powders: Microwave detectors recording incoming (in), passed (tsm), and reflected (ref) radiation power, SP-1 and SP-2 — spectrometers, ADC — analog-to-digital converter

1.2. Reactor

The plasma chemical reactor includes two units. The first unit consists of a duralumin hexagonal housing with a height of 100 mm with a cylindrical cutout in the center with a diameter of 120 mm, in the bottom and top of the housing there are quartz windows for input and output of the microwave pulse of the gyrotron. The two side faces of the casing have optical quartz windows 35 mm in diameter, one of which does not transmit ultraviolet radiation (< 300 nm), as well as two nozzles for gas inlet and pumping.

The second unit is a quartz cylindrical tube with a height of 70 mm and a diameter of 70 mm and a quartz substrate with a cut-out concentric slot for fixing the cylinder. The initial mixture of powders is poured onto a quartz substrate, closed with a quartz cylindrical tube and pressed by means of a Teflon ring inside the block 1.

2. Diagnosis

2.1. Microwave diagnostics

To determine the incident and reflected microwave beam power, three D-407 microwave sensors (*mw detector*, Fig. 2) are used, which operate in linear mode. The microwave radiation power arriving at each measuring detector does not exceed 10^{-4} W.

2.2. Optical diagnostics

Under our conditions there are two characteristic areas: near the powder surface, where the plasma discharge is maintained, and at the top of the reactor, where the flying particles are located, so in the present work we used two spectrometers, one aimed at the bottom of the reactor in the area of the upper surface of the SP-1 powder mixture, and the other — in the upper part of the SP-2 reactor.

Using SP-1, we estimate the temperature of particles in the powder backfill during microwave irradiation and plasma discharge irradiation [10,11]. The particle surface temperature is estimated using Planck's method. The spectral intensity of particle thermal emission is described by the formula

$$I = \varepsilon C_1 \lambda^{-5} / [\exp(C_2/\lambda T) - 1],$$

where ε — spectral emission coefficient, $C_1 = 37418\,\mathrm{W}\cdot\mu\mathrm{m}^4/\mathrm{cm}^2$, $C_2 = 14388\,\mu\mathrm{m}\cdot\mathrm{K}$, λ — wavelength, [μm], T — object temperature, [K]. If the maximum temperature of the object falls within the Wien area $C_2/\lambda T \gg 1$, the formula is converted:

$$\ln(\lambda^5 I) - \ln(\varepsilon C_1) = -C_2/(\lambda T).$$

When using the „grey" model of the $\varepsilon(\lambda, T) = \mathrm{const}$ body, the particle surface temperature will be determined by the slope of the straight line in the guilt coordinates.

For particles in volume, we will be interested in the gas temperature of the flame of burning aluminium particles, the emission from which is mainly due to rotational-vibrational transitions in the two-atom molecule AlO. For this purpose, we calculate the intensity of the AlO molecular bands for the transition $B^2-X^2\Sigma$ (460−530 nm) and fit the calculated spectrum to the experimental spectrum by varying the temperature using the least-squares method [12,13]. The emission intensity in the molecular band $I_{j'j''}$ is found by the formula

$$I_{j'j''} = C_{em} \frac{S_{J',J''} q_{v',v''}}{Q_{rot} v'} (v_{J',J''})^4 e^{-F'J'hc/kT_{rot}} e^{-G'v'hc/kT_{vib}},$$

where C_{em} — emission factor, $S_{J',J''}$ — Holn-London factor, $q_{v',v''}$ — Franck-Condon factor, $v_{J',J''}$ — vibrational transition wave number (v', v''), Q_{rot} — rotational statistical function, F' and G' — vibrational and rotational terms, T_{vib} and T_{rot} — vibrational and rotational temperatures.

A photodetector with a wavelength range of 300 to 550 nm located near the side window of the reactor was used to determine the integral luminosity inside the reactor over time. The bandwidth of the photodetector in the experiments was 80 kHz.

The photo detector and microwave sensors were connected to an ADC (ADC1250, Pulse electric) with a sampling rate of 50 MHz and a bit rate of 12 bit.

The particle scatter is captured on a Phantom VEO710 high-speed camera operating at 7,400 frames per second and shutter speeds up to 1 μs. The chamber is located at a distance of 50 cm at an angle of 60° relative to the plane of the upper window of the reactor. In our geometry, the scale of the image is 185 μm/px. To obtain particle velocity projection information, the images were processed using an original program based on the principle of superimposing two images and tracking the bi-dimensional autocorrelation peak shift of the selected area for two consecutive superimpositions. A Contrastech MARS640-815uc fast color camera operating at 500 frames per second was also installed at the same location to visualize the processes taking place in the reactor throughout the experiment.

3. Results and discussion

The experiment consisted of 15 consecutive microwave pulses of 300 kW power and 6 ms duration, the powder backfill was not replaced throughout the experiment. Characteristic images were chosen to describe the processes inside the reactor, which correspond to the general picture of the dynamics of discharge development and particle dispersion throughout all experiments. Fig. 3 shows sequential photographs taken from the color fast camera. The time interval between frames is 2 ms with a shutter speed of 500 μs. Since the camera has no synchronization with the beginning of the UHF pulse, the T_0 time corresponds to the first frame after the beginning of the UHF pulse. The blue color ($\lambda < 500$ nm) is characteristic of the initial stage of discharge development on the surface of the metal-dielectric powder mixture regardless of the mixture composition. The emission spectrum in this case consists of aluminum atomic lines and molecular bands N_2, CN, O_2, and continuum. As the powder is heated, the intensity of thermal emission increases, as well as the emission of alkali metal lines (NaI, KI), which corresponds to bright yellow emission ($\lambda > 550$ nm). In the frame corresponding to 60 ms after the start of the first frame, the yellow cloud of moving particles inside the quartz cup of the reactor is clearly visible. A sharp luminescence boundary is observed, which disappears with time of the order of 120 ms. The characteristic time of particle cooling down, when there are no bright spots in the image, is of the order of 200 ms.

At camera exposure time 5 μs (Fig. 3, $b1-b4$), the beginning of discharge development can be observed. At time T_0, a spot with a diameter of 30 mm is observed to glow. After 2 ms the luminescence intensity increases and the size of the luminous spot area reaches 50 mm, which corresponds to the diameter of the microwave beam. It

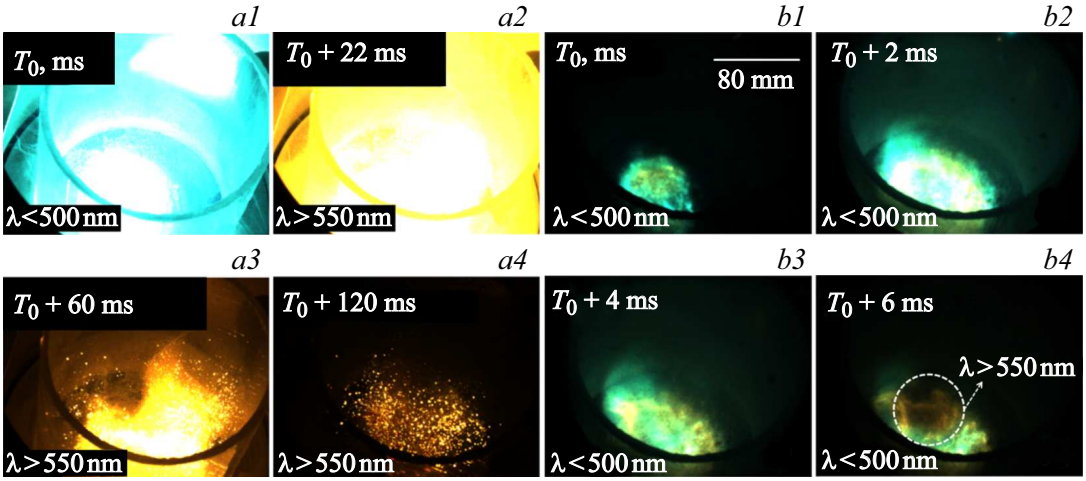

Figure 3. $a1-a4$ — luminous cloud of scattered particles in the air atmosphere (exposure time — 500 μs); $b1-b4$ — development of discharge over the powder surface during the microwave pulse (exposure time — 5 ms).

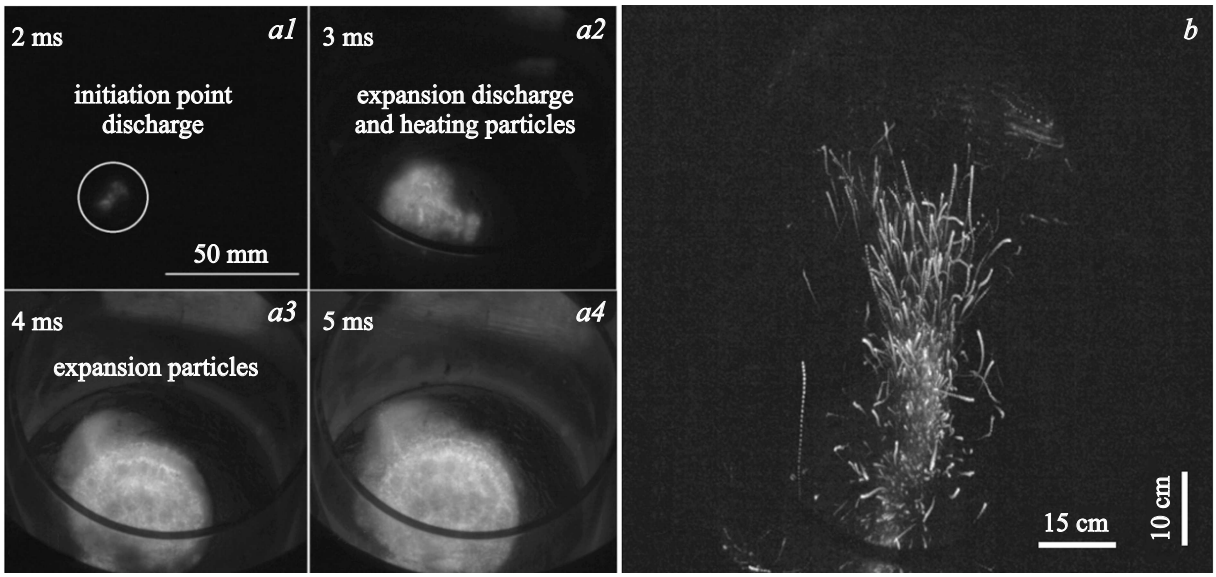

Figure 4. $a1-a4$ — luminous cloud over the surface of the powders during the microwave pulse (exposure time — 5 μs); b — image synthesized from 250 sequentially superimposed frames from 6 to 38 ms after the onset of the microwave pulse

.

can be observed that when the microwave pulse ends at the moment $T_0 + 6$ ms, the plasma discharge is no longer sustained.

Fig. 4 shows footage captured with a Phantom VEO710 high-speed camera with 133 μs exposure and a capture rate of 7300 fps. Pixel intensities are hardware enhanced to better represent particle motion. The camera is synchronized with the onset of the microwave pulse. In 500 μs–2 ms after the onset of the microwave pulse, a local bright point appears on the frames, from which the luminous cloud expands in all directions. From the point of discharge initiation, the particles start to fly away, while the plasma layer continues to form over the surface of the powder mixture. Full formation of the plasma layer occurs 2 ms after discharge initiation. Particle dispersion is predominantly vertical. From the tracks of particles (Fig. 4, $a1-a4$) we can estimate their mean ascent velocity, which ranges from 2 to 5 m/s. In this case, the intensity of the pixels is not related to the intrinsic luminescence of the particles, but is proportional to the time from the beginning of the pulse, so that the darkest points correspond to 6 ms and the brightest to 38 ms.

Fig. 5 shows a view of the time dependence of the microwave detector voltage (tsm) for the elapsed microwave power component and the photodetector for each of the 15 pulses, scaled relative to 2 V (right coordinate axis). In

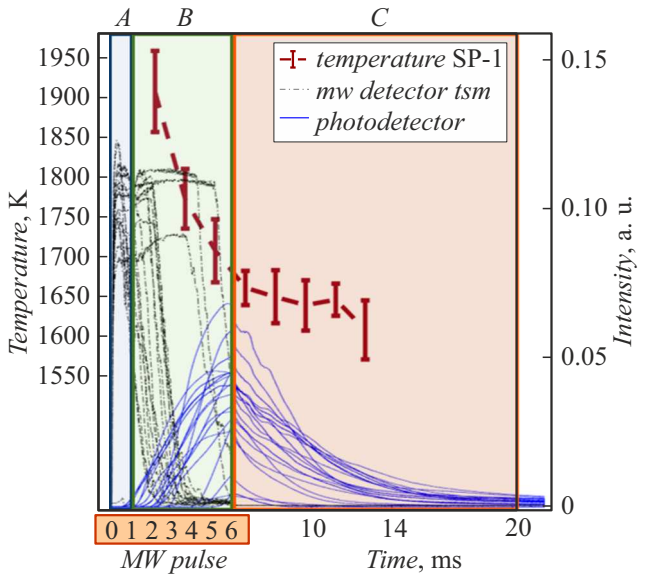

Figure 5. Time dependences of photodetector radiation intensity, microwave detector elapsed signal (tsm) and powder mixture surface temperature

addition, Fig. 5 shows the time dependence of the surface temperature of the SP-1 powder mixture. The obtained spectra from the lower(SP-1) and upper (SP-2) parts of the plasma-chemical reactor, normalized to the maximum intensity in a series of pulses and corrected for the sensitivity of each spectrometer, are shown in Fig. 6, 7.

Based on the experiments performed and the results obtained, the following conclusions can be drawn. The whole particle synthesis process can be divided into three characteristic phases, which are defined by key physico-chemical processes (phase A, B and C in Fig. 5). All times are from the beginning of the microwave pulse.

Phase A (0−1 ms) is characterized by physical processes only: absorption and scattering of microwave energy on powder mixture particles, initiation of surface plasma discharge.

The signal drop of the past microwave detector (tsm) is due to the absorption of microwave beam power in the plasma discharge. The characteristic delay time before discharge initiation is of the order of 500 μs for the first 7−8 pulses. The increase in the delay in the other pulses is due to the processes of reduction of the metallic phase in the powder mixture, due to which a longer pulse duration is required to fulfil the conditions of discharge ignition. Heating of the powder mixture starts at the centers of discharge initiation and spreads throughout the powder (Fig. 3).

The phase B (1−6 ms) is characterized by active physic-ochemical transformations: melting of powder mixture particles, ignition of metal particles, transfer of matter between individual particles.

After initiation of the discharge it is necessary time for heating of powder particles, which we can estimate by the beginning of growth of the photodetector signal, which on average lags by 500 μs from the beginning of absorption of microwave energy in the discharge. During this time, the surface temperature of the powder mixture reaches values between 1850 and 1950 K. These temperatures are well above the melting point of aluminium 950 K, but remain less than the melting point for aluminium oxide 2310 K. However, it is known that the phase transition temperature can be underestimated if nanoparticles [14] are heated. Thus, the temperature maximum in the powder can be limited by the processes of vaporization of the metallic phase and melting of the oxide phase. From 3 ms after the beginning of microwave pulse, the complete absorption of microwave power of gyrotron (Fig. 5) is observed up to the end of pulse, it means that the whole energy of microwave pulse can be transferred to powder mixture through plasma discharge. At the same time, the particle surface temperature starts to decrease as the absorption of radiation in the discharge increases. In such a case, the only way to cool the powder mixture is to fly the particles from the upper layers. Accordingly, in the process of maintaining the discharge, we can distinguish two areas: the first contains the discharge and the powder mixture, and the second — the heated particles flying out. In this case, heated metal particles after overcoming the discharge area fall into a strongly oxidizing medium, which in our experiment is air at atmospheric pressure. The metal particles are ignited in this environment. The characteristic calculated flame temperature of aluminium particles (Fig. 8) in the upper part of the SP-2 reactor corresponds to the range from 3500 to 4000 K both during and after the end of the microwave pulse.

In contrast to the original particles, the particles interacting with the discharge consist mainly of either rounded Al_2O_3 particles (Fig. 9, b, c), or agglomerates of oxide and metal microparticles (Fig. 9, a). The size of metal inclusions in the agglomerates ranges from 1 to 10 μm.

Since no metallic particles outside the agglomerates were detected in the synthesis products, we conclude that almost all of the flying aluminium particles undergo ignition.

The characteristic combustion products of aluminium particles are translucent spheres (Fig. 9, b), on the surface of which cracks in the oxide shell are also observed (Fig. 9, c), the size of such particles is comparable to the size of the original aluminium particles and ranges from 10 to 80 μm (Fig. 9, b, c).

Particle combustion is a negative factor affecting the amount of synthesis products. In this case, particle combustion is an exothermic reaction, which in turn can contribute to the melting of metal particles to form agglomerates (Fig. 9, a). In order to show that the energy put into the plasma discharge is sufficient to melt aluminium particles, we make the following estimate.

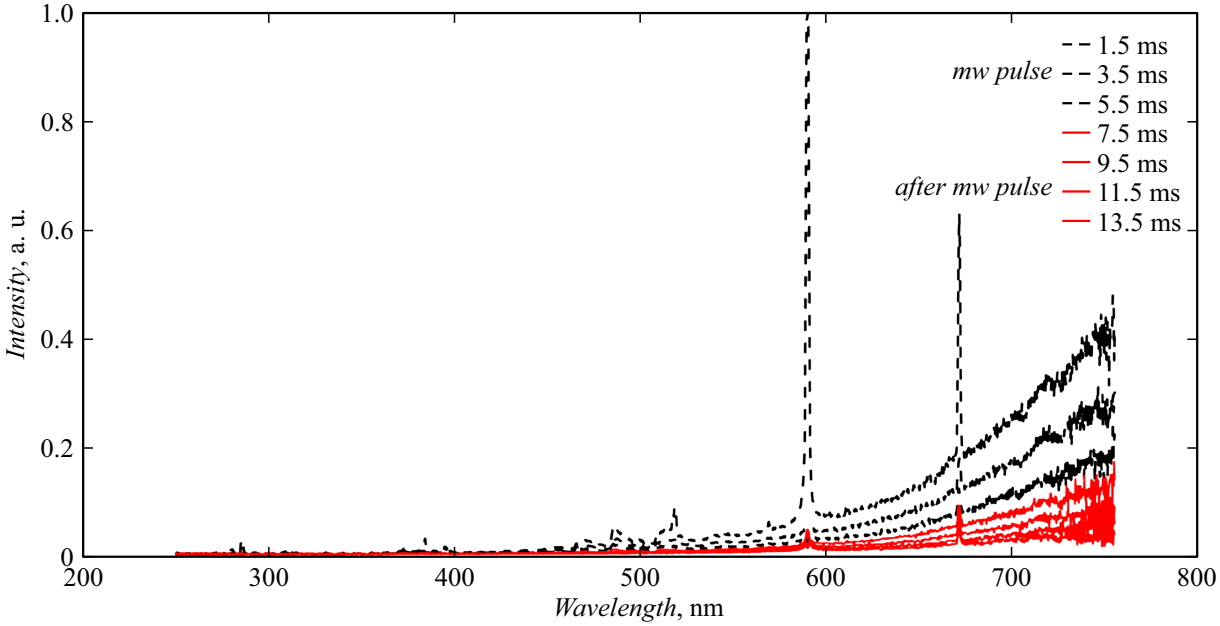

Figure 6. Characteristic SP-1 spectrum from the bottom of the plasma chemical reactor

.

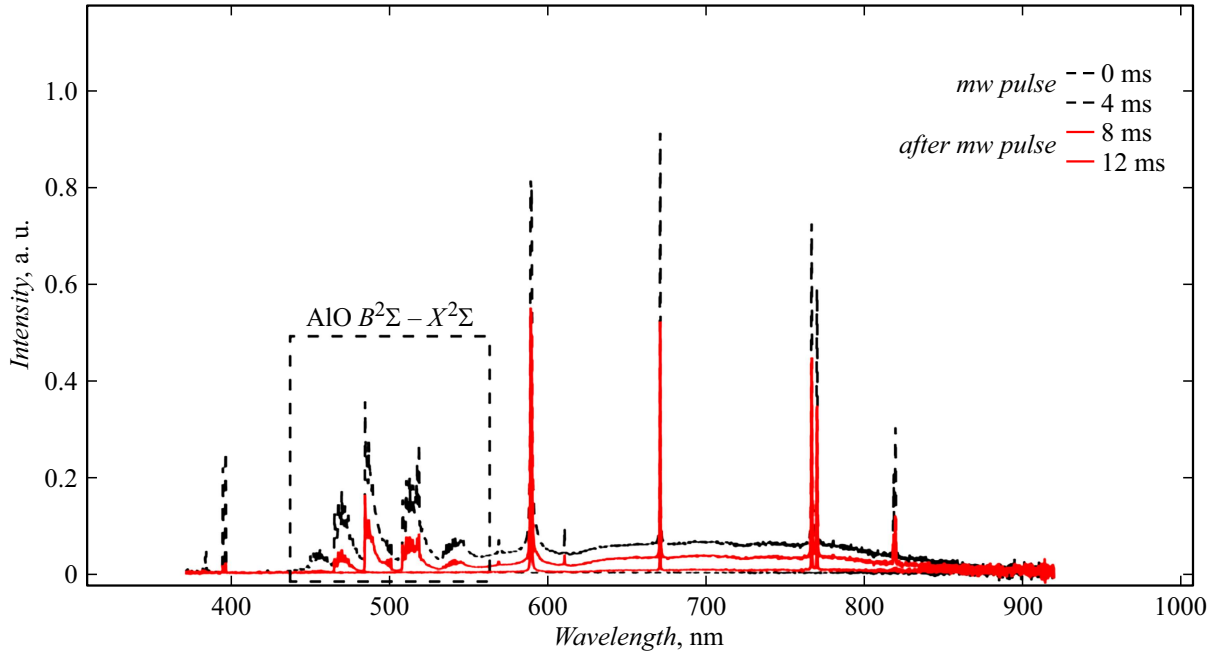

Figure 7. Characteristic SP-2 spectrum from the top of the plasma chemical reactor

.

The specific energy transferred by a microwave pulse during 6 ms for a 50 mm diameter beam is $E = 37.5\,\mathrm{J/cm^2}$. Let us take into account that the microwave energy absorption in the powder mixture is small because most of it is made up of aluminium oxide particles.

Then the power invested in the discharge will correspond to the power in the microwave beam. To heat one aluminium particle of diameter $10\,\mu$m from 300 to 950 K, taking into account the constancy of density, heat capacity and phase transition energy during melting, it is necessary to expend an amount of energy equal to $3 \cdot 10^{-6}$ J. Let us assume that the coefficient of conversion of microwave energy into thermal energy by means of plasma discharge corresponds to 0.1 (this value is chosen on the basis of works [15,16]), then in recalculation of microwave beam energy on the cross-section of the particle

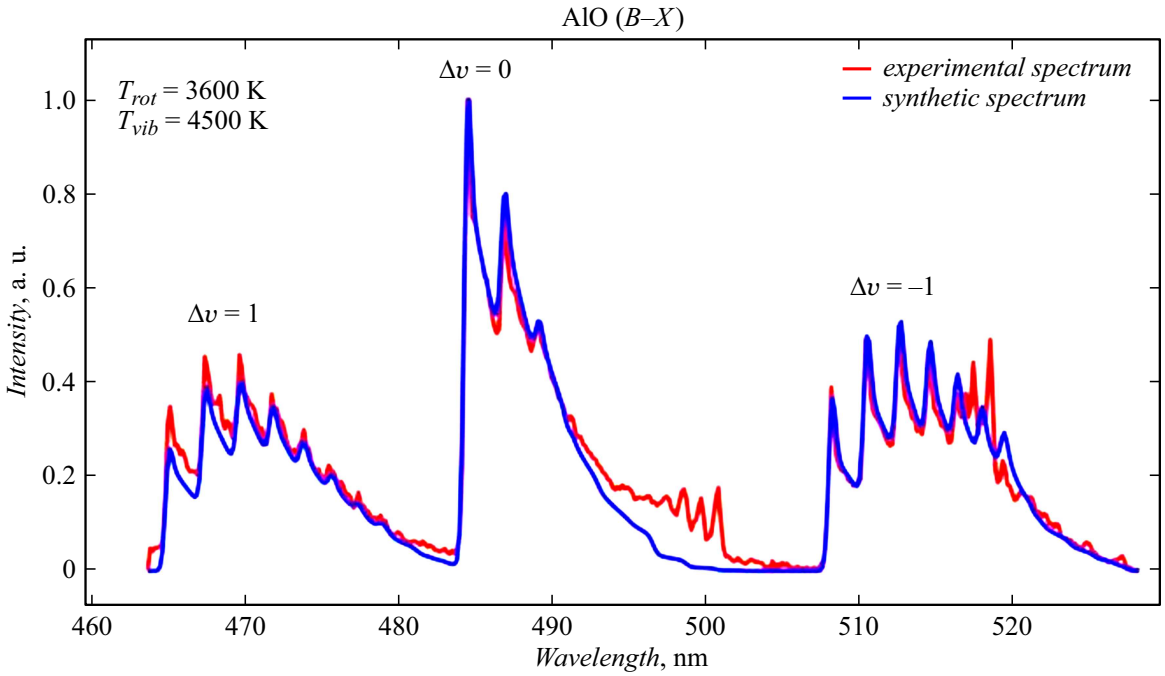

Figure 8. Recorded and calculated emission spectrum of AlO using SP-2 during microwave discharge

.

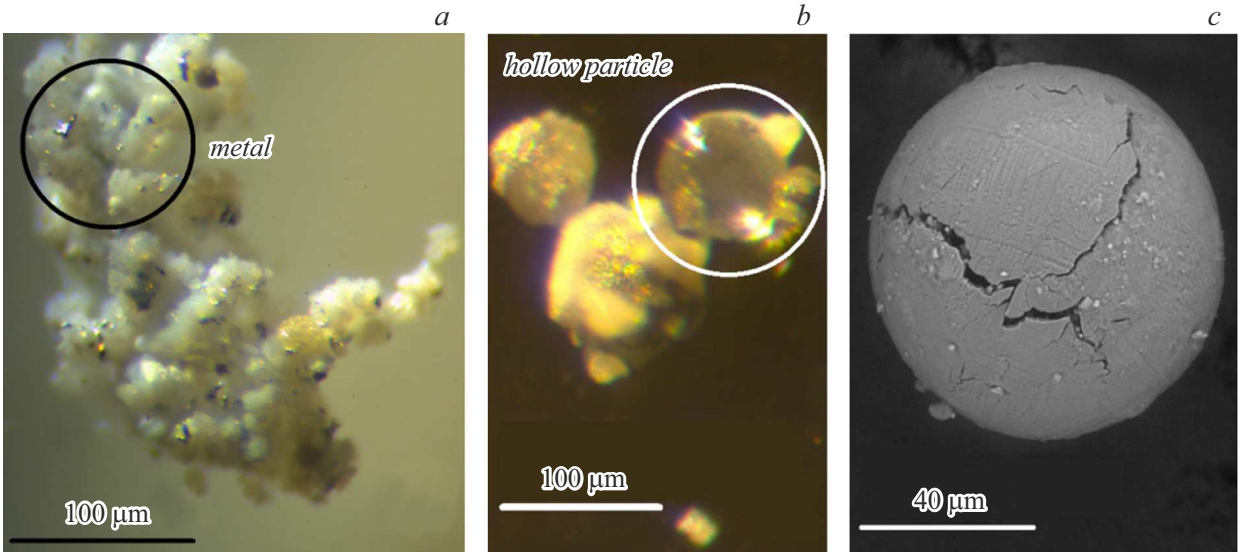

Figure 9. *a* — optical image of synthesized particles after the experiment; *b* — SEM image; *c* — optical image of burnt aluminium particles found in the synthesis products

.

we obtain the value of the invested energy equal to $1.8 \cdot 10^{-6}$ J, which by order of magnitude corresponds to the necessary energy for complete melting of the aluminium particle.

Since particle motion is observed in our experiment, it is also necessary to estimate the formation of metal microdroplets on the oxide surface resulting from the crushing of large (more than 10 μm) aluminium droplets as they rise vertically through the Weber and Ognesorg number ratio. The viscosity and density for aluminium at a melting point of 950 K can be taken from the work [17] for a liquid aluminium particle of diameter 10 μm moving in a medium of temperature $T < T_{mel}$ at a velocity of 5 m/s. The calculated value of Weber number is We $\ll 1$ with Ognesorg number Oh = 0.004. Consequently, a large droplet undergoes only slight deformations [18] (an increase in linear size of less than 5%) and cannot break into smaller droplets.

The phase C (> 6 ms) is characterized by relaxation of combustion processes and radiative cooling of particles in the reactor.

After the microwave pulse, the signal intensity from the photodetector decreases exponentially and is less than 10% of the maximum intensity at 14–20 ms after discharge initiation. This can be explained by a decrease in the fraction of burning particles, resulting in a decrease in the intensity of molecular bands, which is also confirmed by the results of the SP-2 spectrometer (Fig. 7). The reduction time of the photodetector signal, the intensity of molecular bands on SP-2, and the integrated intensity on the high-speed camera frames correspond to a time range of 10 to 20 ms.

These times correspond to the duration of combustion of aluminium particles of size 10–100 μm in the air atmosphere, which, according to [9], ranges from 10 to 100 ms. It is also worth noting, that at this point, the calculated flame temperature has a value above 3000 K, which also indicates that the particles continue to burn in the upper part of the reactor. After 100 ms only heated oxide particles remain in the upper part of the reactor, which can hang in the volume for some time, precipitate on the walls of the quartz cup, or return to the surface of the powder, forming a new top layer.

Conclusion

The interaction process of microwave gyrotron pulse with a mixture of Al/Al_2O_3 powders under normal conditions in an air atmosphere has been experimentally investigated. All stages of development of this process — from initiation of plasma discharge to particle dispersal are considered.

The ignition effect of micro-sized aluminium particles in interaction with a plasma discharge was found. It is shown that the conditions of particle ignition in our experiment weakly affect the temperature and duration of combustion.

The combustion products of aluminium, which return to the surface after dispersal, reduce the amount of initial metal in the powder mixture, which affects the initiation of the plasma-chemical discharge by reducing the amount of metal particles.

The particles interacting with microwave radiation consist mainly of more rounded compared to the original particles Al_2O_3 (10–80 μm). It was shown that among them, characteristic products of aluminium combustion in an air atmosphere were found to be hollow translucent spheres with the presence of cracks in the oxide shell. In addition, large particles (more than 200 μm) of complex shaped aluminium oxide with micro-sized inclusions of metallic aluminium (less than 10 μm) located on its surface were found.

Conflict of interest

The authors declare that they have no conflict of interest.

References

[1] J.P. Yasnó, R.F.K. Gunnewiek, R.H.G.A. Kiminami. Adv. Powder Technol., **30** (7), 1348 (2019). DOI: 10.1016/j.apt.2019.04.010
[2] A. Goldstein, A. Goldenberg, Y. Yeshurun, M. Hefetz. J. Am. Ceram. Soc., **91** (12), 4141 (2008). DOI: 10.1111/j.1551-2916.2008.02788.x
[3] J.H. Kim, J.K. Kim, Y.C. Kang. Appl. Surf. Sci., **523**, 146470 (2020). DOI: 10.1016/j.apsusc.2020.146470
[4] Y. Hu, H. Ding, C. Li. Particuology, **9** (5), 528 (2011). DOI: 10.1016/j.partic.2011.06.003
[5] A.B. Haugen, I. Kumakiri, C. Simon, M-A. Einarsrud. J. Europ. Ceramic Society, **31** (3), 291 (2011). DOI: 10.1016/j.jeurceramsoc.2010.10.006
[6] N.S. Akhmadullina, N.N. Skvortsova, V.D. Stepakhin, E.M. Konchekov, A.A. Letunov, Y.F. Kargin, A.A. Konovalov, O.N. Shishilov. J. Phys.: Conf. Ser., **1347** (1), 012089 (2019). DOI: 10.1088/1742-6596/1347/1/012089
[7] G.M. Batanov, N.K. Berezhetskaya, V.D. Borzosekov, L.D. Iskhakova, L.V. Kolik, E.M. Konchekov, A.A. Letunov, D.V. Malakhov, F.O. Milovich, E.A. Obraztsova, E.D. Obraztsova, A.E. Petrov, K.A. Sarksyan, N.N. Skvortsova, V.D. Stepakhin, N.K. Kharchev. Plasma Phys. Rep., **39**, 843 (2013). DOI: 10.1134/S1063780X13100024
[8] G.M. Batanov, N.K. Berezhetskaya, I.A. Kossyi, A.N. Magunov, V.P. Silakov. Eur. Phys. J. Appl. Phys., **26** (1), 11 (2004). DOI: 10.1051/epjap:2004016
[9] M.W. Beckstead. Fizika Goreniya i Vzryva, **41** (5), 55 (2005). DOI: 10.1007/s10573-005-0067-2 [in Russian]
[10] A.N. Magunov. Nauchnoe Priborostroenie, **20** (3), 22 (2010). [in Russian].
[11] E.V. Voronova, A.V. Knyazev, A.A. Letunov, V.P. Logvinenko, N.N Skvortsova, V.D. Stepakhin. Phys. Atom. Nucl., **84** (10), 1761 (2021). DOI: 10.1134/S1063778821090374
[12] S. Acquaviva, Spectrochim. Acta Part A: Molecular and Biomolecular Spectroscopy, **60** (8–9), 2079 (2004). https://doi.org/10.1016/j.saa.2003.10.040.
[13] X. Bai ,V. Motto-Ros, W. Lei, L. Zheng, J. Yu, Spectrochim. Acta Part B: Atomic Spectroscopy, **99**, 193 (2014). DOI: 10.1016/j.sab.2014.07.004
[14] P. Puri, V. Yang. J. Phys. Chem. C., **111** (32), 11776 (2007). DOI: 10.1021/jp0724774
[15] G.A. Askaryan, G.M. Batanov, I.A. Kossyy. Pisma v ZhTF, **15** (8), 18 (1989) (in Russian).
[16] G.A. Askarian, G.M. Batanov, N.K. Berezhetskaya, S.I. Gritsinin, I.A. Kossyy, I.M. Raevsky. Pisma v ZhETF **29** (706), (1979). (in Russian).
[17] M.J. Assael, K. Kakosimos, R.M. Banish, J. Brillo, I. Egry, R. Brooks, P.N. Quested, K.C. Mills, A. Nagashima, Y. Sato, W.A. Wakeham. J. Phys. Chem. Ref. Data, **35**, 285 (2006). DOI: 10.1063/1.2149380
[18] Z. Dai, G.M. Faeth. Intern. J. Multiphase Flow, **27**, 217 (2001). DOI: 10.1016/S0301-9322(00)00015-X

Translated by Y.Deineka